Published in final edited form as:
J Comp Neurol. 2012 March 1; 520(4): 756–769. doi:10.1002/cne.22773.

Cone Outer Segment Extracellular Matrix as Binding Domain for Interphotoreceptor Retinoid-Binding Protein

Mary Alice Garlipp[1,2,3,4], **Kevin R. Nowak**[2,4], and **Federico Gonzalez-Fernandez**[1,2,3,4,5,*]

[1]Graduate Program in Neuroscience, School of Medicine and Biomedical Sciences, State University of New York, Buffalo, New York 14209

[2]Ira G. Ross Eye Institute Research Center, Department of Ophthalmology, School of Medicine and Biomedical Sciences, State University of New York, Buffalo, New York 14209

[3]Research Service and Division of Anatomic Pathology, Veterans Administration Western New York Healthcare System, Buffalo, New York 14215

[4]State University of New York Eye Institute, Buffalo, New York 14209

[5]Department of Pathology and Anatomical Sciences, School of Medicine and Biomedical Sciences, State University of New York, Buffalo, New York 14209

Abstract

Cones are critically dependent on interphotoreceptor retinoid-binding protein (IRBP) for retinoid delivery in the visual cycle. Cone-dominant vertebrates offer an opportunity to uncover the molecular basis of IRBP's role in this process. Here, we explore the association of IRBP with the interphotoreceptor matrix (IPM) of cones vs. rods in cone dominant retinas from chicken (*Gallus domesticus*), turkey (*Meleagris gallopavo*), and pig (*Sus scrofa*). Retinas were detached and fixed directly or washed in saline prior to fixation. Disassociated photoreceptors with adherent matrix were also prepared. Under 2 mM $CaCl_2$, insoluble matrix was delaminated from saline washed retinas. The distribution of IRBP, as well as glycans binding peanut agglutinin (cone matrix) and wheat germ agglutinin (rod/cone matrix), was defined by confocal microscopy. Retina flat mounts showed IRBP diffusely distributed in an interconnecting, lattice-like pattern throughout the entire matrix. Saline wash replaced this pattern with fluorescent annuli surrounding individual cone outer segments. In isolated cones and matrix sheets, IRBP colocalized with the peanut agglutinin binding matrix glycans. Our results reveal a wash-resistant association of IRBP with a matrix domain immediately surrounding cone outer segments. The cone matrix sheath may be responsible for IRBP-mediated cone targeting of 11-*cis* retinoids.

Keywords

chicken; cones; retina; photoreceptor; cone matrix sheath; interphotoreceptor matrix; interphotoreceptor retinoid-binding protein (IRBP); proteoglycans; peanut agglutinin (PNA); wheat germ agglutinin (WGA); turkey; pig; cone visual cycle

*CORRESPONDENCE TO: Federico Gonzalez-Fernandez, MD, PhD, Research Service, Veterans Affairs Medical Center, Buffalo, New York 14215. fg23@buffalo.edu.

Remarkably, the eye is able to discriminate incremental stimuli over light intensities from a moonlit night to a bright, sunny day. The ability of the retina to function over this nine log unit range is largely due to its duplex structure, consisting of rods and cones (Perlman and Normann, 1998). Both photoreceptor classes capture light photons through the isomerization of 11-*cis* to all-*trans* retinal, which is then reisomerized and returned to the outer segments through the retinoid cycle (Lamb and Pugh, 2004; McBee et al., 2001). Cones, which support daytime vision, require a markedly higher flux of 11-*cis* retinoid compared with rods.

How are 11-*cis* retinoids efficiently targeted to the cone outer segments in the presence of rods, which collectively have a greater outer segment surface area? First, cones, but not rods, can utilize 11-*cis* retinol generated from the Müller glia (Mata et al., 2002). Second, mechanisms could exist to target visual cycle retinoids to the cones. Such a mechanism could involve the unique extracellular matrix surrounding the cone outer segments, known as the “cone matrix sheath.”

Little is known about the function of cone matrix sheaths except that they are specialized regions of the interphotoreceptor matrix (IPM) (Blanks et al., 1988; Hageman and Johnson, 1987; Johnson and Hageman, 1991; Johnson et al., 1986). The IPM consists of 1) an insoluble, lace-like network of components distributed throughout the extracellular space between the photoreceptors, retinal pigment epithelium (RPE), and Müller cells; 2) specialized domains located along the interface between the IPM and surrounding cone outer and inner segments (photoreceptor matrix sheaths); and 3) soluble components bound to the matrix and distributed within the matrix interstices (Hollyfield, 1999; Hollyfield et al., 1998). The insoluble IPM, with its cone matrix sheaths, and bound molecules can be delaminated from the retina as delicate sheets. The matrix is thought to support RPE–retina interactions, including adhesion, photoreceptor stability, and exchange of growth factors and nutrients, such as visual cycle retinoids (Hageman and Kuehn, 1998; Mieziewska, 1996).

The major soluble protein component of the IPM is a 145-kDa glycolipoprotein termed “interphotoreceptor retinoid-binding protein” (IRBP; Gonzalez-Fernandez, 2003; Gonzalez-Fernandez and Ghosh, 2008). IRBP consists of four homologous “modules,” each of ~300 amino acids. It is a member of the crotonase/C-terminal processing protease family, whose members bind hydrophobic ligands in diverse settings. Structural and site-directed mutagenesis studies have defined a putative retinol binding site (Gonzalez-Fernandez et al., 2009). Mutation of a highly conserved salt bridge in the scaffold of the retinoid-binding site is associated with autosomal recessive retinitis pigmentosa (den Hollander et al., 2009). Retinitis pigmentosa is a group of hereditary retinal degenerations characterized by impaired dark adaptation, night blindness, and loss of midperipheral visual field, often leading to blindness (de Maziere et al., 1996; Periasamy et al., 1999). Structural studies of IRBP suggest the presence of conserved charged surface domains that represent putative docking sites for matrix and/or a cell surface receptor (Loew and Gonzalez-Fernandez, 2002). IRBP also contains RHAMM (receptor for HA-mediated motility)-type hyaluronan binding motifs, suggesting an interaction with the matrix scaffold (Hollyfield, 1999).

Through an unknown mechanism, IRBP promotes the release of all-*trans* retinol from the outer segments (Qtaishat et al., 2005; Tsina et al., 2004; Wu et al., 2007) and its delivery to the RPE (Okajima et al., 1989). IRBP also promotes the release of 11-*cis* retinol from the RPE (Carlson and Bok, 1992; Edwards and Adler, 2000) and its return to the outer segments (Jin et al., 2009). Recent studies suggest an important role of IRBP in the cone visual cycle (Jin et al., 2009; Parker and Crouch, 2010; Parker et al., 2009, 2011). The chicken retina provides a useful system to define the molecular basis of these processes (Muniz et al., 2009; Trevino et al., 2005). Interestingly, the expression of the chicken *IRBP* ortholog is light-dependant. The protein accumulates within the IPM and contains a signal peptide followed by four homologous modules, each ~300 amino acid residues in length, in keeping with the structure of tetrapod *IRBPs* (Stenkamp et al., 2005). It is possible that IRBP distinguishes between the different visual cycle retinoids to deliver the appropriate retinoid to the correct cell through tailored receptor docking domains (Gonzalez-Fernandez et al., 2007; Lin et al., 1997).

The present study was designed to determine whether IRBP associates with regions of the IPM. We characterized the distribution of IRBP that remains bound in saline washed retinas and delaminated IPM. We found a previously unrecognized affinity of IRBP for the cone matrix sheath. This finding may help to explain how visual cycle retinoids are efficiently exchanged at cone outer segments.

MATERIALS AND METHODS

Animals and retina isolation

This research was approved by the Veterans Affairs Institutional Animal Care and Use Committee. Retinas were isolated from adult, light-adapted animals [chickens (*Gallus domesticus*), turkeys (*Meleagaris gallopavo*), and swine (*Sus scrofa*)] and were not sorted by sex. The ratio of cones to rods in turkeys (3:1) is similar to that in chickens (Hamel, 2007; Hart et al., 1999; Meyer and May, 1973). In pigs, the ratio is 1:3 (centrally) (Braekevelt, 1983; Gerke et al., 1995). Chickens and turkeys were killed between 7 AM and 10 AM by exsanguination and decapitated at two local farms (Wendel Poultry Farm, Concord, NY, and HLW Acres, Attica, NY). The heads were then light-protected and brought back to the laboratory on ice within 2 hours of slaughter. Eyes were enucleated in the dark with the aid of infrared night vision goggles. After removal of the extraocular muscles, the eyes were placed in 500 ml ice-cold chicken Ringer's (120 mM NaCl, 5.1 mM KCl, 2.75 mM $CaCl_2$, 1.25 mM $MgSO_4$, 1.25 mM KH_2PO_4, 25 mM $NaHCO_3$, 10 mM glucose, 20 mM HEPES pH 7.4). Ten to twelve heads were usually processed per collection. The anterior segment was removed by a circumferential limbal incision, and the retina-eyecups were submerged under Ringer's (seven eyecups per 15 ml). Retinal detachments were also performed in the dark under an infrared stereomicro-scope. Swine were slaughtered at a local farm (D.H. Cloy & Sons) between 7 AM and 10 AM. The enucleated eyes were light-protected and brought back to laboratory on ice within 1 hour of slaughter. Eyes were bisected with a razor blade and retinas detached under 10 mM phosphate, 1 mM $CaCl_2$, 1 mM $MgCl_2$, 25 mM HEPES, pH 7.4 (PBS), at 4°C.

Detached retinas were treated in two ways. 1) “Unwashed” retinas were detached directly under fixative (freshly prepared 4% paraformaldehyde in PBS for 30 minutes). 2) After initial dissection in Ringer's, “washed” retinas were detached under saline and subsequently washed for 2–3 minutes in three changes of 10 ml saline prior to fixation. The formaldehyde solution was always freshly prepared from paraformaldehyde.

Antibody and lectin characterization

We used an anti-bovine mouse monoclonal antibody (mAb F7) generously provided by Dr. Jack Saari (University of Washington). The secondary antibody Alexa conjugates and lectins were purchased from Molecular Probes (Eugene, OR).

MAb F7 is specific for IRBP in a variety of species in both immunohistochemistry and Western blot analysis. Bovine IRBP, the antigen to which mAb F7 was generated against (Table 1), was purified as previously described (Saari et al. 1985). MAb F7 hybridoma cell lines were established, isolated, and screened using techniques similar to those previously described (Gaur et al., 1990). On Western blot analysis of total soluble bovine retinal proteins, mAb F7 recognizes a single band comigrating with purified bovine IRBP (Jack Saari, unpublished observations). Polyclonal antibovine IRBP sera also recognizes a single band with an Mr of 145 kDa corresponding to the known electrophoretic mobility of native bovine IRBP (Bunt-Milam and Saari, 1983). MAb F7 is specific for bovine IRBP at a dilution of 1:500 (Salvador-Silva et al., 2005) and shows no cross-reactivity with RPE microsomes (Nawrot et al., 2004). In chicken retina, mAb F7 has been used to define the distribution of IRBP by immunofluorescence on cryostat sections at 1:1,000 (Fischer et al., 1999, 2008) and tissue flat mounts at 1:500 (Stenkamp et al., 2005).

Peanut agglutinin (PNA) and wheat germ agglutinin (WGA) are useful markers for rod and cone IPM domains, respectively. PNA (from *Arachis hypogaea*) which is specific for galactosyl (β-1,3) N-acetylgalactosamine, was used at 50 μg/ml. WGA (from *Triticum aestivum*) binds N-acetylglucosamine and N-acetylneuraminic acid and was used at 20 μg/ml. At these working concentrations, PNA and WGA have been shown to bind mammalian cone and rod/cone-associated IPM glycans, respectively (Braekevelt, 1983; Hart et al., 1999; Johnson and Hageman, 1991; Johnson et al., 1986; Mieziewska et al., 1991; Perlman and Normann, 1998). Although PNA has not been as extensively studied in nonmammalian retinas, it has been shown to be specific for cones in chickens, teleosts, amphibians, and lampreys (Blanks and Johnson, 1984; Ishikawa et al., 1989; Rohlich and Szel, 2000; Stenkamp et al., 1998; Zhang et al., 1994). Lyophilized Alexa Fluor conjungates, PNA-488 (catalog No. L-21409), WGA-647 (catalog No. W-32466), and WGA-555 (catalog No. W-32464) were reconstituted to 1 mg/ml in PBS, aliquoted, and stored at –20°C until use.

Indirect immunofluorescence of IRBP in retina flat mounts

Fixed turkey, chicken, and pig retinas were washed once in 10 ml PBS. They were then blocked for 30 minutes in 0.1% goat serum in 0.5% Tween in PBS (PBST), pH 7.4, at 23°C. Next, the retinas were gently washed in three changes of 10 ml PBST for 3 minutes each. MAb F7 anti-IRBP incubations were at 1:500 in PBST overnight at 4°C. Controls consisted

of retinas processed without primary antibody. The retinas were again washed in three changes of PBST and incubated with 1:500 goat anti-mouse IgG-647 in PBST overnight at 4°C. Goat anti-mouse IgG-647 Flour conjugate was used as the secondary antibody (catalog No. A-21235). Finally, the retinas were washed in three changes of PBST and incubated at 4°C overnight in 50 μg/ml PNA-488. Care was taken during preparation of flat mounts not to distort the normal in situ orientation of the photoreceptors. Retinas were oriented with photoreceptors facing upward in ProLong Gold AntiFade (Molecular Probes) under a coverslip raised from the slide surface with strips of cut No. 1.5 coverslips. Finally, the edges were sealed with wax (one-third lanolin, one-third paraffin, one-third vaseline).

Immuno- and lectin labeling of isolated living cones

Truncated isolated photoreceptors consisting of outer segments with attached inner segments are useful models for rod and cone cells (Biernbaum and Bownds, 1985). They can be prepared by mechanical agitation of the retina. Frog rod inner segments/rod outer segments (RIS/ROS) have been used to study the interaction of IRBP with outer segments (Wu et al., 2007). However, there is less experience in the literature with the preparation of cone outer segments/cone inner segments (CIS/ COS) except for that in teleosts (Pagh-Roehl et al., 1992). We are not aware of any study isolating CIS/COS from avians. To isolate cells with intact IPM, we adapted a protocol for chicken outer segment isolation used in iodopsin purification (Matsumoto and Yoshizawa, 1982). The centrifugation step was omitted to minimize disruption of the cells and their matrix. We performed the antibody and lectin incubations on the intact retina to allow washing of the photoreceptors without centrifugation. Our protocol is described in detail below.

After dissection in PBS buffer (see above), isolated retinas were washed in three 10 ml changes of PBS and blocked for 30 minutes at 23°C in 0.1% goat serum in PBS. Retinas were then incubated with mAb F7 anti-IRBP and/or lectin for 1 hour at 23°C. MAb F7 was used at 1:500, followed by 1:500 goat anti-mouse IgG-647. PNA-488 and WGA-647 were used at 50 μg/ml and 20 μg/ml, respectively. Retinas were washed with one 10 ml change of PBS between probes. To prepare the CIS/COS and cell clusters, retinas were gently triturated in PBS (1 retina per ml) with a 4 mm tip plastic transfer pipette. The retina was then slowly triturated four times inside a 2 ml microfuge tube. With avoidance fo the visible retina fragments, 20 μl of the CIS/COS suspension was quickly transferred using a large-orifice 200 μl pipette tip (Fisher, Fair Lawn, NJ; catalog No. 02-707-134) to subbed slides (we found that 1% porcine gelatin 300 bloom in 0.1% chromium potassium sulfate provided the best overall adhesive properties for the cells, retinas, and matrix used in our study). The cells were allowed to adhere to the subbed slides for 10 minutes. After this, the slides were gently flooded with 100 μl freshly prepared 4% paraformaldehyde. No attempt to further manipulate or wash the cells was made; they were directly coverslipped under fixative and sealed with wax. Confocal microscopy was performed within 12 hours.

Isolation of IPM sheets

We adapted the hypotonic incubation method used in bovine and human retina to isolate insoluble IPM from turkey and chicken retina (Hollyfield, 1999; Johnson and Hageman 1991; Johnson et al., 1986). To our knowledge, this is the first time that this method has

been applied in avians. Freshly isolated retinas were washed three times in 15 ml PBS, and the insoluble IPM wasw delaminated as continuous sheets from the retina under chilled 2 mM $CaCl_2$. After a 6- to 9-minute soak, the matrix sheets began to lift slightly off the underlying retina. Jeweler's forceps were used to aid in the separation. The matrix sheets were difficult to remove, because the retina tends to curl. To ameliorate this, the retina was cut into smaller pieces before delaminating. The detached matrix sheets were then carefully transferred to subbed slides (1% porcine gelatin 300 Bloom in 0.1% chromium potassium sul-fate) and mounted by allowing the sheets nearly to dry (~15 minutes, or until just tacky) on the slide before fixation. Mounted sheets were fixed by gently dipping in freshly prepared 4% paraformaldehyde in PBS for 5 minutes, dried, and held in closed, light-protected boxes at 4°C until examined (generally within 48 hours).

IRBP indirect immunofluorescence in isolated IPM sheets

Matrix sheet flat mounts were prepared as described above. Slides were initially rinsed twice in PBST to remove residual fixative, and blocked for 30 minutes at 23°C in 0.1% goat serum in PBS. Slides were then rinsed once with PBST and incubated with mAb F7 anti-IRBP at 1:500 in PBST for 1 hour at 23°C in a humidity chamber. After primary antibody incubation, slides were rinsed twice with PBST and incubated in 1:500 goat anti-mouse IgG-647 in PBST for 1 hour. After antibody incubation, the matrix sheets were washed once in PBST. For triple labeling, PNA-488 at 50 μg/ml and WGA-555 at 20 μg/ml (in that order) were incubated with the sheets for 1 hour. After lectin incubations, slides were rinsed once with PBST, mounted, and sealed with wax.

Confocal microscopy and image analysis

Confocal microscopy was performed on a Zeiss Axiovert 200 inverted microscope equipped with a Zeiss LSM-510 Meta NLO laser scanner (laser lines 488, 568, and 647 nm). Optical sections were taken at 0.5 μm. Images were collected using Zeiss LSM 510 Imager 4.2. Raw images collected from the LSM were imported into Adobe Photoshop 4.0 and adjustments made in the “Levels” palette, moving the black-point and white-point sliders to flank the histogram in the red, green, and blue channels. Areas of overlap in red–green fluorescence images appear yellow. Supporting Information figures of red–green fluorescence were converted into magenta–green using the “Channels” palette. The “Red” channel was copied and pasted onto the “Blue” channel, thus replacing the red with magenta, and areas of overlap appear white in converted images (see Supporting Information).

RESULTS

To study the association of IRBP within the IPM of the cone-dominant retina, we began our studies using chicken retinal flat mounts. The cone array is clearly seen by the various colored oil droplets on flat mount preparations (Fig. 1A). Three cone subtypes are recognized by their distinctive oil droplets and cellular morphology (Fig. 1B; Meyer and Cooper, 1966). Chicken retina flat mounts are an excellent system in which to visualize the cone array.

To assess the distribution of IRBP in the chicken IPM, the retinas were detached directly under fixative and the distribution of IRBP characterized by immunofluorescence (Fig. 2). In Figure 2A–D, the retinas were detached directly under fixative (“unwashed”). Here, the distrubtion of IRBP appeared as an interconnected lace-like network (Fig. 2B). The cone oil droplets can be appreciated by differential interference contrast microscopy (DIC) in flat mounts (arrow, Fig. 2A) and in cross-sectional orientations (arrow, Fig. 2D). Under immunofluorescence, the oil droplets appear as dark regions in the immunofluorescence panels. Figure 2C (merged DIC and fluorescence) localizes oil droplets at the centers of many of these unstained regions. The diameter of dark regions (“holes”) depends on the level of optical sectioning and cone subtype; note the staggered relative positions of outer and inner segments in Figure 1B. Smaller holes, which often lack a central oil droplet, correspond to outer segments. In contrast, larger regions often do contain oil droplets; they delineate inner segment regions. These results indicate that, in unwashed retinas, IRBP is distributed throughout the IPM in an uninterrupted, continuous lace-like network.

To determine the effect of saline wash on IRBP's association with the IPM, we washed the retinas three times prior to fixation. Immunofluorescence showed that the lace-network was replaced by a distinctive subpattern (Figs. 2F, 3). This new pattern was dominated by individual separate annuli of varying diameter. The more diffuse matrix staining previously observed between photoreceptors was much less apparent, consistent with loss of IRBP from these regions (compare with Fig. 2B). The wash-resistant IRBP encircled all the cone cells and was more prominent around outer segments than inner segments (see oblique section, Fig. 3C). In contrast, the intervening matrix stained only lightly (asterisk in Fig. 3D). Delicate filament-like densities extending radially from the IRBP annuli could often be appreciated (arrowheads, Fig. 3D), with some appearing to bridge annuli. The larger annuli sometimes contained oil droplets that emitted a green autofluorescence. The smallest annuli, which lacked oil droplets, delimited outer segments. In the case of double cones, the optical section captured adjacent outer and inner segments (arrow, Fig. 3A,D), which appeared to share a common annular segment. Taken together, these results indicate that there is a wash-resistant fraction of IRBP, that is more tightly bound to a pericellular domain immediately encircling the cone cells.

To extend these studies to other cone-dominant vertebrates, we examined the distribution of IRBP and PNA binding glycans in the turkey and pig retina (Figs. 4, 5). PNA was selected as a matrix marker, because this lectin has been shown to be a cone matrix marker (Blanks et al., 1988; Johnson and Hageman, 1991; Johnson et al., 1986). The distribution of IRBP and PNA-binding glycans were compared in the retina of chicken (Fig. 4A–C), turkey (Fig. 4D–F), and pig (Fig. 5). As with chicken, a wash-resistant IRBP was observed in the turkey and pig retina flat mounts. The pattern in turkey and pig was somewhat different from that in chicken. Whereas the chicken typi cally showed separate annuli, in turkey and pig the annuli tended to merge with each other. However, for all three species, IRBP always colocalized with PNA. Little IRBP was detected that did not colocalize with PNA. These results suggest that IRBP has a high affinity for the cone associated IPM.

To evaluate further whether IRBP binds to the cone-associated IPM, we performed similar experiments on living photoreceptor clusters and CIS/COS preparations (Figs. 6, 7).

By using a more limited and gentler trituration procedure than is generally employed to prepare RIS/ROS, we found that it was possible to obtain living CIS/COS and rod/cone clusters that retain visible cone matrix sheath. Under DIC, the sheath can be appreciated surrounding the outer segments as a flocculent material, which tapers around the inner segments (arrowhead, Fig. 6A,D). This matrix contained PNA and WGA binding glycans (Fig. 6B,E). The ability to retain matrix, which to our knowledge has never been described, suggests a useful method to study the cone matrix sheath in isolated living cells. In the cell cluster shown in Figure 7A–C, IRBP colocalized with the outer segment PNA-positive cone matrix sheath (arrow; note that the included rod outer segment is not labeled, arrowhead). Similarly, in the double cone (Fig. 7D–F), IRBP was sequestered in the PNA-positive matrix (arrow) but is restricted to the matrix immediately surrounding the outer segment (Fig. 7C,F). The PNA binding domain extended beyond that of IRBP to the IPM associated with the inner segment. These data indicate that IRBP binds to a subdomain of the cone matrix sheath, which is restricted to the outer segment.

To assess whether IRBP is bound to isolated IPM, we prepared detached sheets of insoluble matrix. Here, we adapted the low ionic strength incubation method employed to isolate insoluble mammalian IPM from retina to isolate the insoluble matrix (Hollyfield et al., 1989; Johnson et al., 1986). Delamination of insoluble matrix was accomplished by soaking the retina in 2 mM $CaCl_2$. This treatment swells the matrix, allowing it to be carefully peeled away from the retina as delicate sheets. The sheets were then carefully transferred to subbed slides for staining as described in Materials and Methods. Figure 8 shows such a preparation of isolated insoluble chicken matrix sheet immobilized and probed for IRBP and PNA-binding glycans. The panels show a lattice-like network (asterisk), with scattered cone matrix sheath profiles (arrows). Compared with the retinal flat mounts shown in Figures 3–5, the cone sheaths are separated farther from one another because of the matrix swelling. IRBP was largely concentrated in the cone matrix sheaths and was less abundant in the intersheath areas. We extended these observations to compare the distribution of both WGA and PNA with that of IRBP. Figure 9 shows isolated turkey insoluble matrix triple labeled for each of these markers. IRBP was present in the cone matrix sheath (arrows) but not in the rod-associated matrix (arrowhead, Fig. 9A). PNA and WGA showed a different matrix distribution (Fig. 9B,C). WGA staining enhanced matrix domains (asterisk) that appeared to extend between cone matrix sheaths. These results show that the association of IRBP with the cone matrix sheath persists in delaminated matrix sheet delamination.

DISCUSSION

Since its discovery more than 3 decades ago, it has been generally assumed that IRBP is not significantly bound to the retina, explaining why it is effectively obtained by saline irrigation (Adler and Evans, 1983; Liou et al., 1982; Pfeffer et al., 1983). Most of the experience comes from rod-dominant animals such as cattle, from which IRBP is often purified (Adler et al., 1990; Fong et al., 1984; Saari et al., 1985). Here, for cone-dominant species, we revisit the assumption that IRBP is only loosely associated with the retina. Our main finding is the existence of a wash-resistant IRBP fraction that binds to the extracellular matrix immediately surrounding the cone outer segments. This previously unrecognized

affinity accounts for its apparent sequestration in the cone matrix sheath and may be especially relevant to understanding IRBP's role in the cone visual cycle.

IRBP is distributed within the IPM in a light-dependent manner, suggesting physiologically important interactions with components of the matrix and/or the cells bordering the subretinal space (Uehara et al., 1990). However, because IRBP is very abundant in the matrix, it is difficult to distinguish the sites to which it is binding. To circumvent this problem, we washed the retina in saline, allowing removal of the excess IRBP. This strategy has been useful to localize IRBP in RPE endocytic vesicles and phagosomes (Cunningham and Gonzalez-Fernandez, 2003). In that study, IRBP was also detected by Western blot analysis in washed retina. However, the distribution of the wash-resistant IRBP was not characterized by immunohistochemistry. Instead, it was assumed that this IRBP represents newly synthesized protein within the photoreceptor Gogli system (Carter-Dawson and Burroughs, 1992b) and/or a separate pool located within photoreceptor multivesicular bodies (Hollyfield et al., 1985a,b). To our knowledge, a wash-resistant extracellular IRBP has never been described in the literature.

Our findings, which suggest that the association of IRBP with the cone outer segments represents a binding of IRBP to a specific component(s) of the cone matrix sheath, is consistent with previous descriptions in the literature. Immunogold electron microscopy has established that IRBP is present in the rod-associated IPM (Gonzalez-Fernandez and Ghosh, 2008; Gonzalez-Fernandez et al., 1998; Hauswirth et al., 1992). In monkey (Carter-Dawson and Burroughs, 1992a) and ground squirrel (Anderson et al., 1986) retinas, immunoelectron microscopy has shown that IRBP is present in the cone matrix sheath.

In the present study, immunofluorescence patterns of retina flat mounts, isolated cones, and isolated IPM sheets indicate a nonwashable fraction of IRBP localized to the outer segment domain of the cone matrix sheath. Double labeling of isolated turkey cone cells and flat mounts of chicken and pig retinas reveals colocalization of extracellular PNA-binding glycans with IRBP. IRBP showed less association with WGA binding glycans. In avian species, there may be more overlap between the PNA and WGA binding domains compared with that in mammals, where PNA-binding is specific for cone matrix sheaths, and WGA-binding is specific for rod-associated matrix. However, in dog, cat, and mouse retina, WGA stains both rods and cones. In contrast, PNA is more specific for cones (Mieziewska et al., 1991). PNA blots have shown species differences in the molecular weight and quantity of the retinal lectin binding glycans (Hageman and Johnson, 1986). Our studies extend previous immunohistochemical observations in the chicken retina (Anderson et al., 1986; Stenkamp et al., 2005) by showing that the association of IRBP with the cone matrix sheath represents binding of IRBP to an unidentified component(s) of this distinct matrix domain. A wash-resistant cone associated IRBP has also been demonstrated in Xenopus. (Garlipp and Gonzalez-Fernandez, 2010, 51:1896, ARVO abstract).

Because daytime vision requires higher rates of chromophore photoisomerization and regeneration compared with scotopic conditions, cones must compete with rods for limited 11-*cis* chromphore (Wang and Kefalov, 2011). However, cones are more sensitive than rods to conditions of limited 11-*cis* retinal (Samardzija et al., 2009). This probably is due to their

higher spontaneous rate of chromophore dissociation (Kefalov et al., 2005), and the fact that rod outer segments are larger and typically more numerous than those of cones. Therefore, a central question is: How do cones effectively compete for 11-*cis* chromophore? One mechanism may be the ability of cones to utilize 11-*cis* retinol produced by the Müller cells (Mata et al., 2002). Rods, which cannot oxidize this retinoid, are dependent on 11-*cis* retinal generated by the RPE. Although this enzymatic compartmentalization provides a protected source of 11-*cis* chromophore for cones, it does not explain how 11-*cis* retinol and 11-*cis* retinal are efficiently targeted to the cone outer segments in the presence of the greater rod outer segment surface area. Recent studies point to an essential role of IRBP in the cone visual cycle, and its absence causes cone degeneration resulting from inadequate delivery of 11-*cis* retinal to the cone outer segments (Jin et al., 2009; Parker et al., 2009, 2011). However, the underlying mechanisms through which IRBP targets 11-*cis* chromophore to the cones are largely unknown.

In summary, we show for the first time that the sequestration of IRBP around the cones is not due simply to an increased volume of the extracellular matrix around the outer segments compared with that of rods, but is due to an affinity of IRBP for a component(s) of the cone matrix sheath itself. This anatomical domain could allow IRBP to interface directly with the cone outer segments through its specialized matrix sheath. This unique microenvironment may provide cones with ready access to 11-*cis* retinol and 11-*cis* retinal, and enhance the efficiency of all-*trans* retinol removal at the cone outer segments. Ongoing experiments in our laboratory are aimed at defining the matrix components responsible for this IRBP binding. The large size of the cone-dominant avian retina will facilitate isolation and characterization of the molecular components responsible for this interaction.

Supplementary Material

Refer to Web version on PubMed Central for supplementary material.

Acknowledgments

The authors thank Dr. Wade Sigurdson for his helpful suggestions during the course of this research, Dr. Jack Saari for the mAb F7 anti-IRBP antibody, Herman and Laura Weber for providing the chicken and turkey tissues, and Dave and Joyce Cloy for providing the pig tissues for this research.

Additional Supporting Information may be found in the online version of this article.

Grant sponsors: National Institutes of Health R01 EY09412 (to F.G-F.); Merit Review Award I01BX007080 from the Biomedical Laboratory Research and Development Service of the Veterans Affairs Office of Research and Development; Grant (to F.G-F.); National Institutes of Health R24 EY 016662 core instrumentation grant; An unrestricted Research Grant from Research to Prevent Blindness to the Department of Ophthalmology at SUNY at Buffalo; F.G.-F. holds the Ira Gile Ross and Elizabeth Pierce Olmsted Ross Endowed Chair in Ophthalmic Pathology.

LITERATURE CITED

Adler AJ, Evans CD. Rapid isolation of bovine interphotoreceptor retinol-binding protein. Biochim Biophys Acta. 1983; 761:217–222. [PubMed: 6686062]

Adler AJ, Chader GJ, Wiggert B. Purification and assay of interphotoreceptor retinoid-binding protein from the eye. Methods Enzymol. 1990; 189:213–223. [PubMed: 2292937]

Anderson DH, Neitz J, Saari JC, Kaska DD, Fenwick J, Jacobs GH, Fisher SK. Retinoid-binding proteins in cone-dominant retinas. Invest Ophthalmol Vis Sci. 1986; 27:1015–1026. [PubMed: 3721781]

Biernbaum MS, Bownds MD. Frog rod outer segments with attached inner segment ellipsoids as an in vitro model for photoreceptors on the retina. J Gen Physiol. 1985; 85:83–105. [PubMed: 3871471]

Blanks JC, Johnson LV. Specific binding of peanut lectin to a class of retinal photoreceptor cells. A species comparison. Invest Ophthalmol Vis Sci. 1984; 25:546–557. [PubMed: 6715128]

Blanks JC, Hageman GS, Johnson LV, Spee C. Ultra-structural visualization of primate cone photoreceptor matrix sheaths. J Comp Neurol. 1988; 270:288–300. [PubMed: 3379160]

Braekevelt CR. Fine structure of the retinal rods and cones in the domestic pig. Graefes Arch Clin Exp Ophthalmol. 1983; 220:273–278. [PubMed: 6629020]

Bunt-Milam AH, Saari JC. Immunocytochemical localization of two retinoid-binding proteins in vertebrate retina. J Cell Biol. 1983; 97:703–712. [PubMed: 6350319]

Carlson A, Bok D. Promotion of the release of 11-cis-retinal from cultured retinal pigment epithelium by inter-photoreceptor retinoid-binding protein. Biochemistry. 1992; 31:9056–9062. [PubMed: 1390692]

Carter-Dawson L, Burroughs M. Interphotoreceptor retinoid-binding protein in the cone matrix sheath. Electron microscopic immunocytochemical localization. Invest Ophthalmol Vis Sci. 1992a; 33:1584–1588. [PubMed: 1559756]

Carter-Dawson L, Burroughs M. Interphotoreceptor retinoid-binding protein in the Golgi apparatus of monkey foveal cones. Electron microscopic immunocytochemical localization. Invest Ophthalmol Vis Sci. 1992b; 33:1589–1594. [PubMed: 1559757]

Cunningham LL, Gonzalez-Fernandez F. Internalization of interphotoreceptor retinoid-binding protein by the Xenopus retinal pigment epithelium. J Comp Neurol. 2003; 466:331–342. [PubMed: 14556291]

de Maziere AM, Hage WJ, Ubbels GA. A method for staining of cell nuclei in Xenopus laevis embryos with cyanine dyes for whole-mount confocal laser scanning microscopy. J Histochem Cytochem. 1996; 44:399–402. [PubMed: 8601700]

den Hollander AI, McGee TL, Ziviello C, Banfi S, Dryja TP, Gonzalez-Fernandez F, Ghosh D, Berson EL. A homozygous missense mutation in the IRBP gene (RBP3) associated with autosomal recessive retinitis pigmentosa. Invest Ophthalmol Vis Sci. 2009; 50:1864–1872. [PubMed: 19074801]

Edwards RB, Adler AJ. IRBP enhances removal of 11-cis-retinaldehyde from isolated RPE membranes. Exp Eye Res. 2000; 70:235–245. [PubMed: 10655150]

Fischer AJ, Wallman J, Mertz JR, Stell WK. Localization of retinoid binding proteins, retinoid receptors, and retinaldehyde dehydrogenase in the chick eye. J Neurocytol. 1999; 28:597–609. [PubMed: 10800207]

Fischer AJ, Foster S, Scott MA, Sherwood P. Transient expression of LIM-domain transcription factors is coincident with delayed maturation of photoreceptors in the chicken retina. J Comp Neurol. 2008; 506:584–603. [PubMed: 18072193]

Fong SL, Liou GI, Landers RA, Alvarez RA, Bridges CD. Purification and characterization of a retinol-binding glyco-protein synthesized and secreted by bovine neural retina. J Biol Chem. 1984; 259:6534–6542. [PubMed: 6427217]

Gaur VP, De Leeuw AM, Milam AH, Saari JC. Localization of cellular retinoic acid-binding protein to amacrine cells of rat retina. Exp Eye Res. 1990; 50:505–511. [PubMed: 2164945]

Gerke CG, Hao Y, Wong F. Topography of rods and cones in the retina of the domestic pig. Hong Kong Med J1. 1995

Gonzalez-Fernandez F. Interphotoreceptor retinoid-binding protein—an old gene for new eyes. Vis Res. 2003; 43:3021–3036. [PubMed: 14611938]

Gonzalez-Fernandez F, Ghosh D. Focus on molecules: interphotoreceptor retinoid-binding protein (IRBP). Exp Eye Res. 2008; 86:169–170. [PubMed: 17222825]

Gonzalez-Fernandez F, Baer CA, Baker E, Okajima TI, Wiggert B, Braiman MS, Pepperberg DR. Fourth module of Xenopus interphotoreceptor retinoid-binding protein: activity in retinoid transfer

between the retinal pigment epithelium and rod photoreceptors. Curr Eye Res. 1998; 17:1150–1157. [PubMed: 9872537]

Gonzalez-Fernandez F, Baer CA, Ghosh D. Module structure of interphotoreceptor retinoid-binding protein (IRBP) may provide bases for its complex role in the visual cycle—structure/function study of Xenopus IRBP. BMC Biochem. 2007; 8:15. [PubMed: 17683573]

Gonzalez-Fernandez F, Bevilacqua T, Lee KI, Chandrashekar R, Hsu L, Garlipp MA, Griswold JB, Crouch RK, Ghosh D. Retinol-binding site in interphotoreceptor retinoid-binding protein (IRBP): a novel hydrophobic cavity. Invest Ophthalmol Vis Sci. 2009; 50:5577–5586. [PubMed: 19608538]

Hageman GS, Johnson LV. Biochemical characterization of the major peanut-agglutinin-binding glycoproteins in vertebrate retinae. J Comp Neurol. 1986; 249:499–493. [PubMed: 3745505]

Hageman GS, Johnson LV. Chondroitin 6-sulfate glycosaminoglycan is a major constituent of primate cone photoreceptor matrix sheaths. Curr Eye Res. 1987; 6:639–646. [PubMed: 3107909]

Hageman, GS.; Kuehn, MH. Biology of the interphotoreceptor matrix-retinal interface.. In: Marmor, MF.; Wolfensberber, TJ., editors. The retinal pigment epithelium. Oxford University Press; New York: 1998. p. 361-391.

Hamel CP. Cone rod dystrophies. Orphanet J Rare Dis. 2007; 2:7. [PubMed: 17270046]

Hart NS, Partridge JC, Cuthill IC. Visual pigments, cone oil droplets, ocular media and predicted spectral sensitivity in the domestic turkey (Meleagris gallopavo). Vis Res. 1999; 39:3321–3328. [PubMed: 10615498]

Hauswirth WW, Langerijt AV, Timmers AM, Adamus G, Ulshafer RJ. Early expression and localization of rhodopsin and interphotoreceptor retinoid-binding protein (IRBP) in the developing fetal bovine retina. Exp Eye Res. 1992; 54:661–670. [PubMed: 1623951]

Hollyfield JG. Hyaluronan and the functional organization of the interphotoreceptor matrix. Invest Ophthalmol Vis Sci. 1999; 40:2767–2769. [PubMed: 10549633]

Hollyfield JG, Varner HH, Rayborn ME, Bridges CD. Participation of photoreceptor cells in retrieval and degradation of components in the interphotoreceptor matrix. Prog Clin Biol Res. 1985a; 190:171–175. [PubMed: 2864698]

Hollyfield JG, Varner HH, Rayborn ME, Liou GI, Bridges CD. Endocytosis and degradation of interstitial retinol-binding protein: differential capabilities of cells that border the interphotoreceptor matrix. J Cell Biol. 1985b; 100:1676–1681. [PubMed: 4039328]

Hollyfield JG, Varner HH, Rayborn ME, Osterfeld AM. Retinal attachment to the pigment epithelium. Linkage through an extracellular sheath surrounding cone photoreceptors. Retina. 1989; 9:59–68. [PubMed: 2470124]

Hollyfield JG, Rayborn ME, Tammi M, Tammi R. Hyaluronan in the interphotoreceptor matrix of the eye: species differences in content, distribution, ligand binding and degradation. Exp Eye Res. 1998; 66:241–248. [PubMed: 9533850]

Ishikawa M, Watanabe H, Koike Y, Hisatomi O, Tokunaga F, Tonosaki A. Demonstration by lectin cytochemistry of rod and cone photoreceptors in the lamprey retina. Cell Tissue Res. 1989; 256:227–232. [PubMed: 2731214]

Jin M, Li S, Nusinowitz S, Lloyd M, Hu J, Radu RA, Bok D, Travis GH. The role of interphotoreceptor retinoid-binding protein on the translocation of visual retinoids and function of cone photoreceptors. J Neurosci. 2009; 29:1486–1495. [PubMed: 19193895]

Johnson LV, Hageman GS. Structural and compositional analyses of isolated cone matrix sheaths. Invest Ophthal Vis Sci. 1991; 32:1951–1957. [PubMed: 2055688]

Johnson LV, Hageman GS, Blanks JC. Interphotoreceptor matrix domains ensheath vertebrate cone photoreceptor cells. Invest Ophthalmol Vis Sci. 1986; 27:129–135. [PubMed: 3080382]

Kefalov VJ, Estevez ME, Kono M, Goletz PW, Crouch RK, Cornwall MC, Yau KW. Breaking the covalent bond—a pigment property that contributes to desensitization in cones. Neuron. 2005; 46:879–890. [PubMed: 15953417]

Lamb TD, Pugh EN. Dark adaptation and the retinoid cycle of vision. Prog Ret Eye Res. 2004; 23:307–380.

Lin ZY, Li GR, Takizawa N, Si JS, Gross EA, Richardson K, Nickerson JM. Structure–function relationships in interphotoreceptor retinoid-binding protein (IRBP). Mol Vis. 1997; 3:17. [PubMed: 9479008]

Liou GI, Bridges CD, Fong SL, Alvarez RA, Gonzalez-Fernandez F. Vitamin A transport between retina and pigment epithelium—an interstitial protein carrying endogenous retinol (interstitial retinol-binding protein). Vis Res. 1982; 22:1457–1467. [PubMed: 6892133]

Loew A, Gonzalez-Fernandez F. Crystal structure of the functional unit of interphotoreceptor retinoid binding protein. Structure. 2002; 10:43–49. [PubMed: 11796109]

Mata NL, Radu RA, Clemmons RC, Travis GH. Isomerization and oxidation of vitamin a in cone-dominant retinas: a novel pathway for visual-pigment regeneration in day-light. Neuron. 2002; 36:69–80. [PubMed: 12367507]

Matsumoto H, Yoshizawa T. Preparation of chicken iodopsin. Methods Enzymol. 1982; 81:154–160. [PubMed: 7098859]

McBee JK, Palczewski K, Baehr W, Pepperberg DR. Confronting complexity: the interlink of phototransduction and retinoid metabolism in the vertebrate retina. Prog Ret Eye Res. 2001; 20:469–529.

Meyer DB, Cooper TG. The visual cells of the chicken as revealed by phase contrast microscopy. Am J Anat. 1966; 118:723–734. [PubMed: 5334066]

Meyer DB, May HC Jr. The topographical distribution of rods and cones in the adult chicken retina. Exp Eye Res. 1973; 17:347–355. [PubMed: 4765257]

Mieziewska K. The interphotoreceptor matrix, a space in sight. Microsc Res Techniq. 1996; 35:463–471.

Mieziewska KE, van Veen T, Murray JM, Aguirre GD. Rod and cone specific domains in the interphotoreceptor matrix. J Comp Neurol. 1991; 308:371–380. [PubMed: 1865006]

Muniz A, Betts BS, Trevino AR, Buddavarapu K, Roman R, Ma JX, Tsin AT. Evidence for two retinoid cycles in the cone-dominated chicken eye. Biochemistry. 2009; 48:6854–6863. [PubMed: 19492794]

Nawrot M, West K, Huang J, Possin DE, Bretscher A, Crabb JW, Saari JC. Cellular retinaldehyde-binding protein interacts with ERM-binding phosphoprotein 50 in retinal pigment epithelium. Invest Ophthalmol Vis Sci. 2004; 45:393–401. [PubMed: 14744877]

Okajima TI, Pepperberg DR, Ripps H, Wiggert B, Chader GJ. Interphotoreceptor retinoid-binding protein: role in delivery of retinol to the pigment epithelium. Exp Eye Res. 1989; 49:629–644. [PubMed: 2509230]

Pagh-Roehl K, Brandenburger J, Wang E, Burnside B. Actin-dependent myoid elongation in teleost rod inner/outer segments occurs in the absence of net actin polymerization. Cell Motil Cytoskeleton. 1992; 21:235–251. [PubMed: 1581976]

Parker RO, Crouch RK. The interphotoreceptor retinoid binding (IRBP) is essential for normal retinoid processing in cone photoreceptors. Adv Exp Med Biol. 2010; 664:141–149. [PubMed: 20238012]

Parker RO, Fan J, Nickerson JM, Liou GI, Crouch RK. Normal cone function requires the interphotoreceptor retinoid binding protein. J Neurosci. 2009; 29:4616–4621. [PubMed: 19357286]

Parker R, Wang JS, Kefalov VJ, Crouch RK. Interphotoreceptor retinoid-binding protein as the physiologically relevant carrier of 11-cis-retinol in the cone visual cycle. J Neurosci. 2011; 31:4714–4719. [PubMed: 21430170]

Periasamy A, Skoglund P, Noakes C, Keller R. An evaluation of two-photon excitation versus confocal and digital deconvolution fluorescence microscopy imaging in Xenopus morphogenesis. Microsc Res Techniq. 1999; 47:172–181.

Perlman I, Normann RA. Light adaptation and sensitivity controlling mechanisms in vertebrate photoreceptors. Prog Ret Eye Res. 1998; 17:523–563.

Pfeffer B, Wiggert B, Lee L, Zonnenberg B, Newsome D, Chader G. The presence of a soluble interphotoreceptor retinol-binding protein (IRBP) in the retinal interphotoreceptor space. J Cell Physiol. 1983; 117:333–341. [PubMed: 6686234]

Qtaishat NM, Wiggert B, Pepperberg DR. Interphotoreceptor retinoid-binding protein (IRBP) promotes the release of all-trans retinol from the isolated retina following rhodopsin bleaching illumination. Exp Eye Res. 2005; 81:455–463. [PubMed: 15935345]

Rohlich P, Szel A. Photoreceptor cells in the Xenopus retina. Microsc Res Techniq. 2000; 50:327–337.

Saari JC, Teller DC, Crabb JW, Bredberg L. Properties of an interphotoreceptor retinoid-binding protein from bovine retina. J Biol Chem. 1985; 260:195–201. [PubMed: 2981203]

Salvador-Silva M, Ghosh S, Bertazolli-Filho R, Boatright JH, Nickerson JM, Garwin GG, Saari JC, Coca-Prados M. Retinoid processing proteins in the ocular ciliary epithelium. Mol Vis. 2005; 11:356–365. [PubMed: 15928609]

Samardzija M, Tanimoto N, Kostic C, Beck S, Oberhauser V, Joly S, Thiersch M, Fahl E, Arsenijevic Y, von Lintig J, Wenzel A, Seeliger MW, Grimm C. In conditions of limited chromophore supply rods entrap 11-cis-retinal leading to loss of cone function and cell death. Hum Mol Genet. 2009; 18:1266–1275. [PubMed: 19147682]

Stenkamp DL, Cunningham LL, Raymond PA, Gonzalez-Fernandez F. Novel expression pattern of interphotoreceptor retinoid-binding protein (IRBP) in the adult and developing zebrafish retina and RPE. Mol Vis. 1998; 4:26. [PubMed: 9841935]

Stenkamp DL, Calderwood JL, Van Niel EE, Daniels LM, Gonzalez-Fernandez F. The interphotoreceptor retinoid-binding protein (IRBP) of the chicken (Gallus gallus domesticus). Mol Vis. 2005; 11:833–845. [PubMed: 16254552]

Trevino SG, Villazana-Espinoza ET, Muniz A, Tsin AT. Retinoid cycles in the cone-dominated chicken retina. J Exp Biol. 2005; 208:4151–4157. [PubMed: 16244173]

Tsina E, Chen C, Koutalos Y, Ala-Laurila P, Tsacopoulos M, Wiggert B, Crouch RK, Cornwall MC. Physiological and microfluorometric studies of reduction and clearance of retinal in bleached rod photoreceptors. J Gen Physiol. 2004; 124:429–443. [PubMed: 15452202]

Uehara F, Matthes MT, Yasumura D, LaVail MM. Light-evoked changes in the interphotoreceptor matrix. Science. 1990; 248:1633–1636. [PubMed: 2194288]

Wang JS, Kefalov VJ. The cone-specific visual cycle. Prog Ret Eye Res. 2011; 30:115–128.

Wu Q, Blakeley LR, Cornwall MC, Crouch RK, Wiggert BN, Koutalos Y. Interphotoreceptor retinoid-binding protein is the physiologically relevant carrier that removes retinol from rod photoreceptor outer segments. Biochemistry. 2007; 46:8669–8679. [PubMed: 17602665]

Zhang J, Kleinschmidt J, Sun P, Witkovsky P. Identification of cone classes in Xenopus retina by immunocytochemistry and staining with lectins and vital dyes. Vis Neurosci. 1994; 11:1185–1192. [PubMed: 7530991]

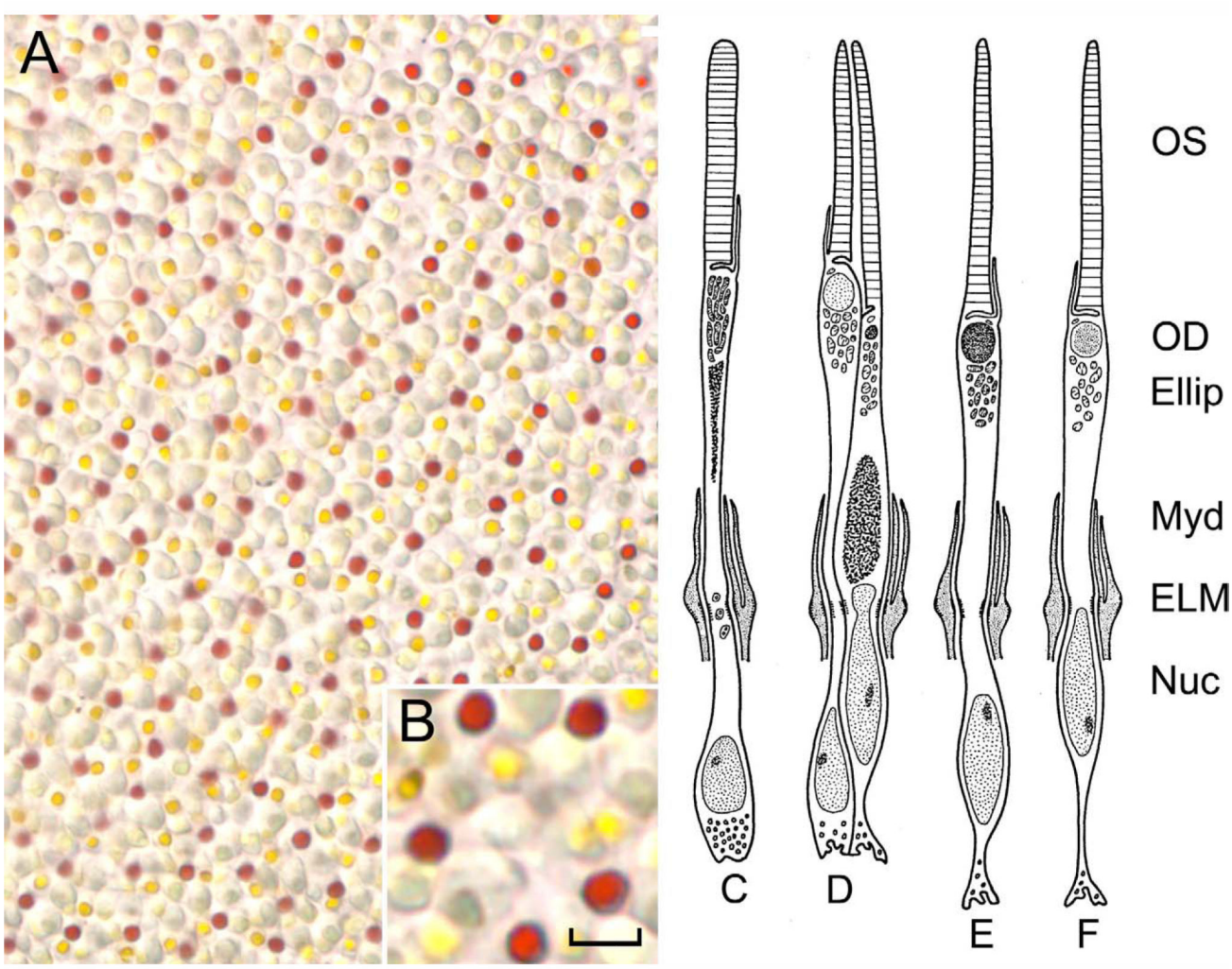

Figure 1.

Chicken photoreceptor subtypes. **A**: The retina flat mount shows the cone cell mosaic with its various colored oil droplets (inset in **B**). There are four visual cells: rod (**C**; 13%), no oil droplet; double cone (**D**; 36%), consisting of larger principal cone with golden-yellow oil droplet, and smaller accessory cone with green-yellow oil droplet; single cone type I (**E**; 25%), dark red oil droplet; single cone type II (**F**; 11%), light colored oil droplet. OS, outer segment; OD, oil droplet, Ellip, ellipsoid; Myd, myoid; ELM, external limiting membrane; Nuc, nucleus. Diagram adapted from Morris and Shorey (J. Comp. Neurol. 129:313–340, 1997) with permission from John Wiley & Sons, Inc. Scale bar = 10 μm in A, 5 μm in B.

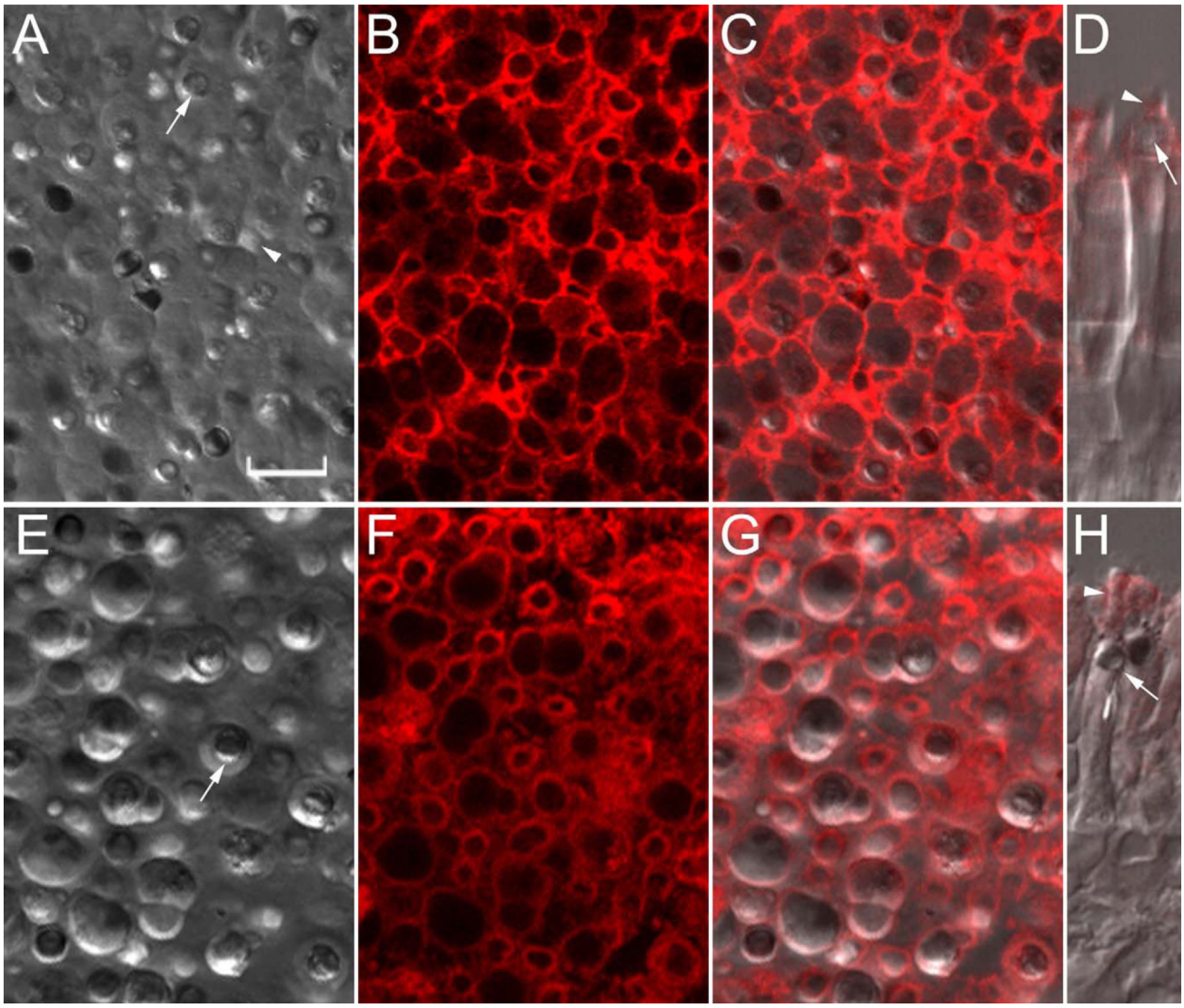

Figure 2.

Effect of saline wash on IRBP distribution. Unwashed chicken retinas were detached directly under 4% paraformaldehyde (**A–D**), or washed retinas were detached under Ringer's saline (**E–H**). Retina flat mounts were probed with mAb F7 anti-IRBP, followed by goat anti-mouse IgG-647. **A,E**: Differential interference contrast microscopy (DIC). **B,F**: Confocal IRBP immunofluorescence (633 nm). **C,G**: Fluorescence merged with DIC. **D,H**: Same tissue following removal from coverslipped slide and reoriented for cross-sections (fuorescence merged with DIC). Oil droplet (arrow), outer segments (arrowhead). A magenta–green copy of this figure is available as Supporting Information Figure 2. Scale bar = 10 μm.

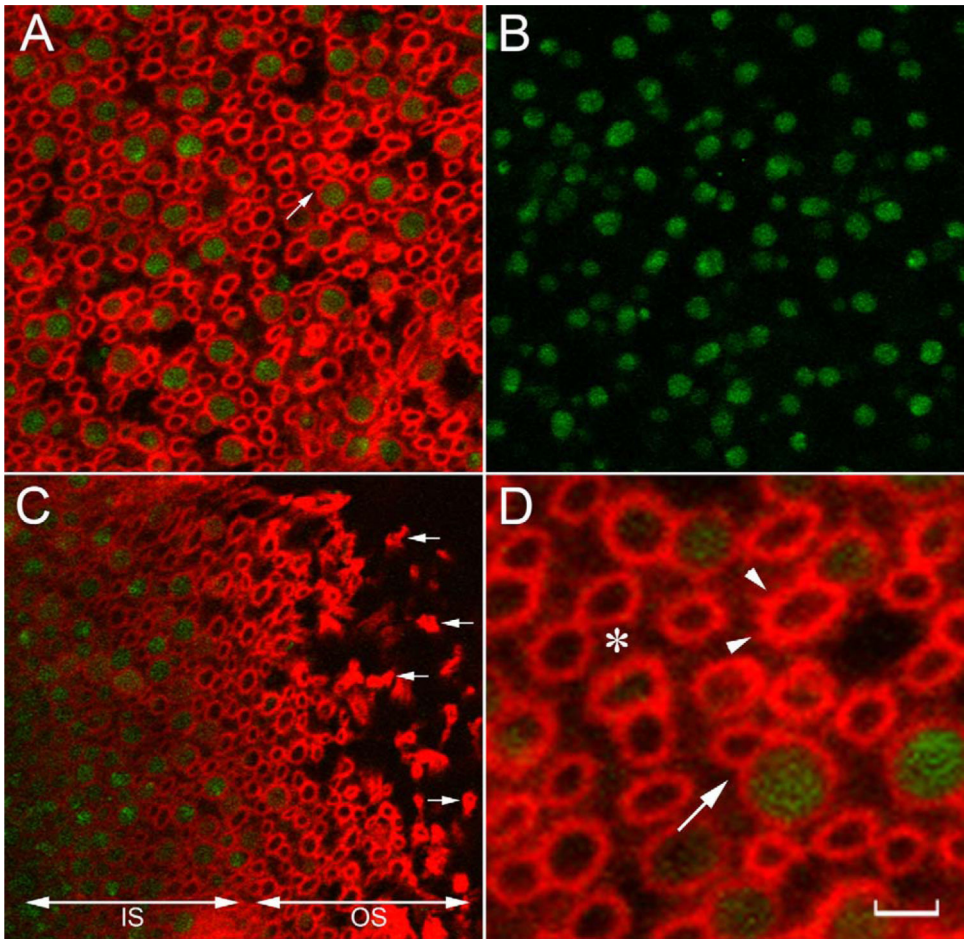

Figure 3.

IRBP distribution in saline washed chicken retina. Retinas were washed three times, flat mounted, and probed with mAb F7 anti-IRBP, followed by goat anti-mouse IgG-647. Overview of merged confocal fluorescence images at 633 nm (red, IRBP) and 488 nm (green, oil droplet autofluorescence). **A**: En face orientation of cone array of IRBP indirect immunofluorescence (arrow, double cone). **B**: En face orientation incubated without primary antibody. **C**: Oblique section showing inner segment (IS) and outer segment (OS) zones. Arrows, distal cone outer segments tips. **D**: Enlargement of marked double-cone region in **A**. Arrowheads, ring-like association of IRBP with cone outer segments; asterisk, region between IRBP cone-associated domains. A magenta–green copy of this figure is available as Supporting Information Figure 3. Scale bar = 3.3 μm in D; 10 μm for A–C.

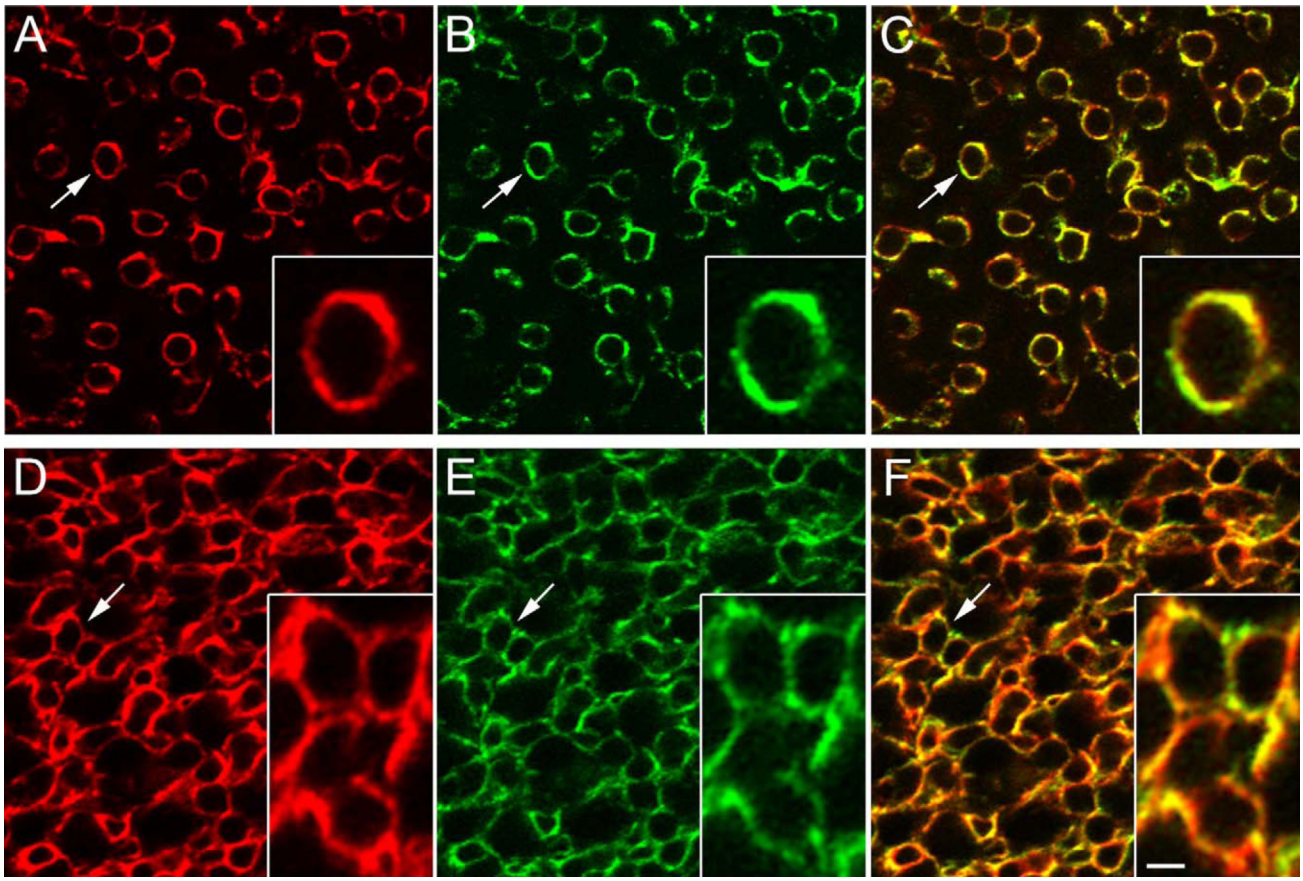

Figure 4.

Localization of IRBP and PNA-binding glycans in chicken (**A–C**) and turkey (**D–F**) retinas. Isolated retinas were probed with mAb F7 anti-IRBP, followed by goat anti-mouse IgG-647 (**A,D**) and PNA-488 (**B,E**). **C,F**: Merged fluorescence. Omission of the primary antibody or PNA-488 showed no fluorescence (data not illustrated). Arrows correspond to cone matrix sheath magnified in insets. A magenta–green copy of this figure is available as Supporting Information Figure 4. Scale bar = 2 μm in insets; 10 μm for **A–F**.

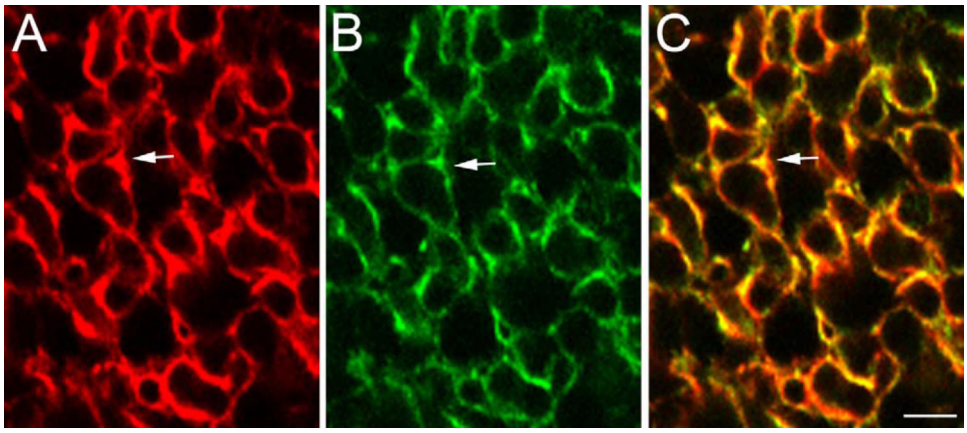

Figure 5.

Localization of IRBP and PNA-binding glycans in the pig retina. Isolated retinas were probed with mAb F7 anti-IRBP, followed by goat anti-mouse IgG-647 (**A**) or PNA-488 (**B**). Merged fluorescence is shown in **C**. IRBP and PNA-binding glycans show strong colocalization (arrow). A magenta–green copy of this figure is available as Supporting Information Figure 5. Scale bar = 10 μm.

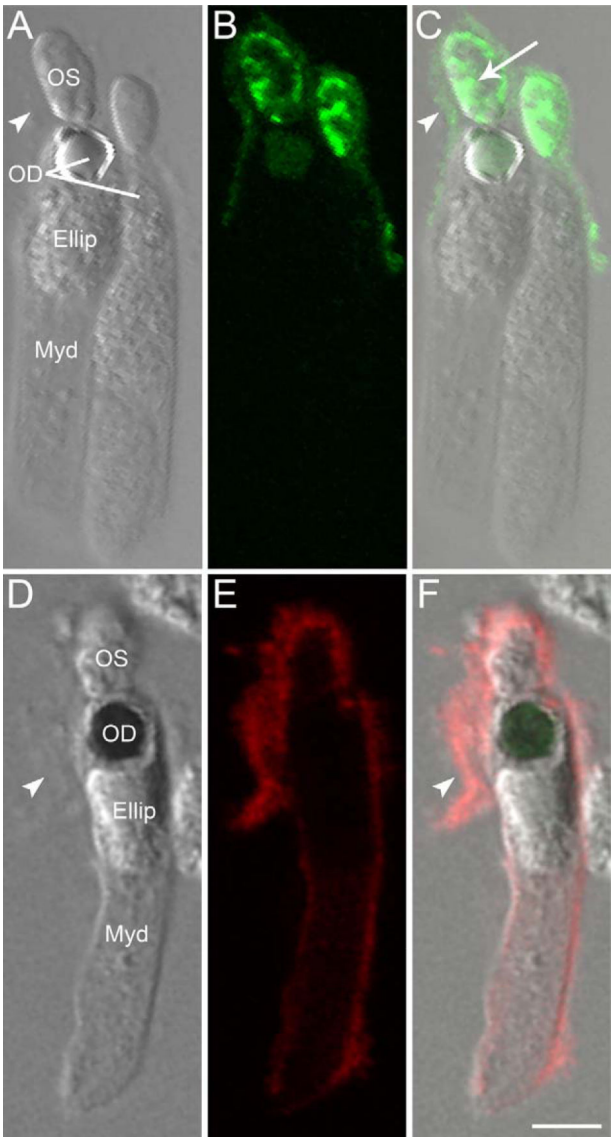

Figure 6.

Isolated turkey cones probed with PNA-488 (**A–C**) or WGA-647 (**D–F**). Washed retinas were incubated with either lectin prior to gentle trituration to generate CIS/COS. **A,D**: Retained cone matrix sheath (arrowheads) is detectable around the outer and inner segments by DIC. **B,E**: Confocal immunofluorescence of PNA-488 and WGA-647 fluorescence, respectively. **C,F**: Merged fluorescence and DIC. OS, outer segment; OD, oil droplets; Ellip, ellipsoid; Myd, myoid; arrow, PNA-positive cone matrix sheath. A magenta–green copy of this figure is available as Supporting Information Figure 6. Scale bar = 5 μm.

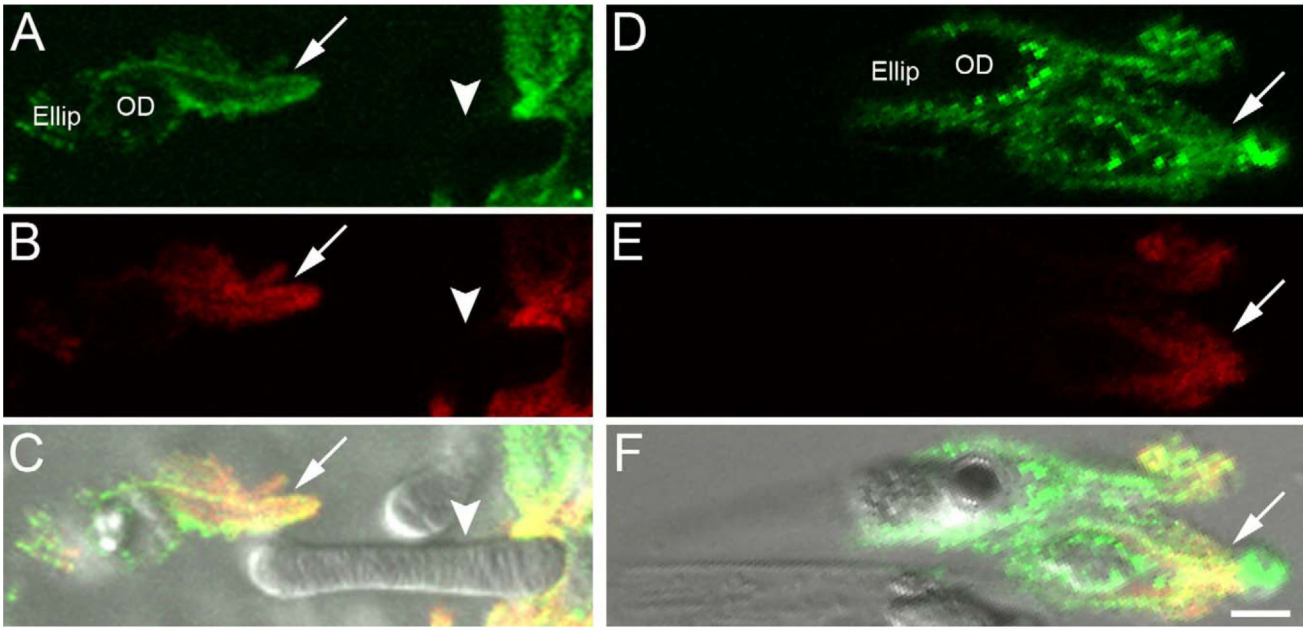

Figure 7.

Localization of IRBP and PNA-binding glycans in dissociated turkey photoreceptors. Washed retinas were incubated with mAb F7 anti-IRBP followed by goat anti-mouse IgG-647. The tissue was then probed with PNA-488 and gently triturated to generate photoreceptor clusters or CIS/COS. **A–C** show a single cone (outer segment marked with arrow) and nearby rod outer segment (arrowhead); **D–F** show a double cone. **A,D**: Cone matrix sheath labeling with PNA-488. **B,E**: IRBP localization within the cone matrix sheath. **C,F**: Merged corresponding fluorescence and DIC images. Note that IRBP colocalization within the cone matrix sheath is restricted to an outer segment subdomain (yellow merged fluorescence). Ellip, ellipsoid; OD, oil droplet. A magenta–green copy of this figure is available as Supporting Information Figure 7. Scale bar = 8.7 μm in **F** (applies to D–F); 5 μm for **A–C**.

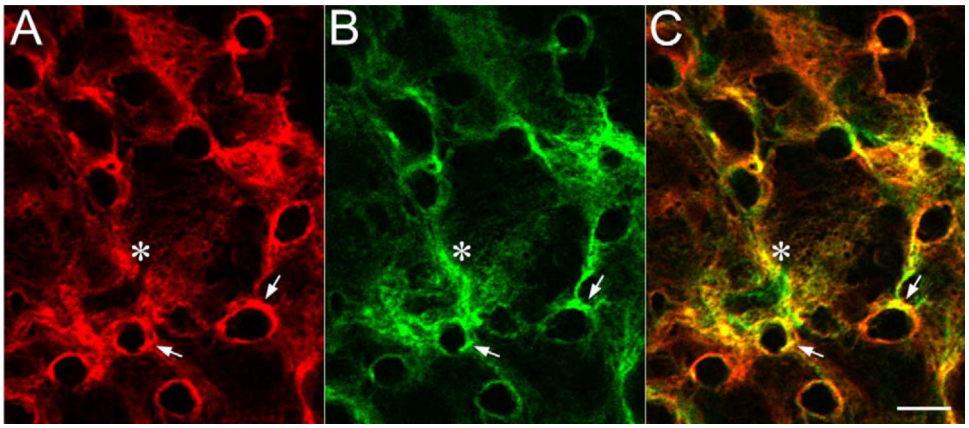

Figure 8.

Localization of IRBP and PNA-binding glycans in isolated chicken IPM. Matrix sheets were delaminated from retinas in 2 mM $CaCl_2$ and mounted onto subbed slides. **A**: Indirect IRBP immunofluorescence using mAb F7 anti-IRBP detected with goat anti-mouse IgG-647. **B**: Distribution of PNA-488-binding glycans. **C**: Merged fluorescence. Asterisk, matrix appearing to bridge between cone matrix sheath structures; arrows, fluorescence colocalization in cone matrix sheaths. A magenta–green copy of this figure is available as Supporting Information Figure 8. Scale bar = 10 μm.

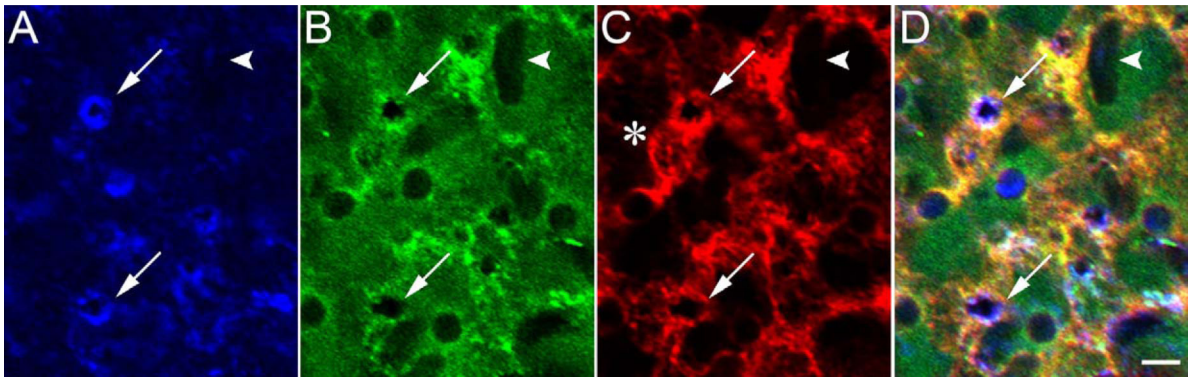

Figure 9.

Localization of IRBP and PNA- and WGA-binding glycans within isolated turkey IPM. The matrix sheet was delaminated from a freshly isolated retina in 2 mM $CaCl_2$ and probed with MAb F7 anti-IRBP followed by goat-anti mouse IgG-647 (**A**), PNA-488 (**B**), and WGA-555 (**C**). **D**: Merged IRBP, PNA, and WGA fluorescence. IRBP immunofluorescence is shown in blue because three fluorophores are used (647-blue, 633 nm; 488-green, 488 nm; 555-red, 561 nm). Asterisk, WGA-positive matrix appearing to bridge nearby cone sheaths; arrows, colocalization of IRBP and PNA/WGA-binding glycans; arrowheads, rod-associated matrix. A magenta–green copy of this figure is available as Supporting Information Figure 9. Scale bar = 5 μm.

TABLE 1

Primary Antibody Used

Antigen	Immunogen	Species in which antibody was raised and source	Dilution used
IRBP	Full-length native purified bovine IRBP	Supernatant from mouse hybridoma; Jack Saari (University of Washington)	1:500